

# 185 MHz Count Rate, 139 dB Dynamic Range Single-Photon Avalanche Diode with Active Quenching Circuit in 130 nm CMOS Technology

Andreas Eisele<sup>[1,2]</sup>, Robert Henderson<sup>[3]</sup>, Bernd Schmidtke<sup>[2]</sup>, Tobias Funk<sup>[2]</sup>, Lindsay Grant<sup>[4]</sup>, Justin Richardson<sup>[3,5]</sup>, Wolfgang Freude<sup>[1,6]</sup>

<sup>[1]</sup>Institute of Photonics and Quantum Electronics (IPQ), Karlsruhe Institute of Technology (KIT), 76131 Karlsruhe, Germany

<sup>[2]</sup>Robert Bosch GmbH, Max-Lang-Strasse 40-46, 70771 Leinfelden, Germany

<sup>[3]</sup>The University of Edinburgh, Institute for Integrated Micro and Nano Systems, Edinburgh, U.K.

<sup>[4]</sup>STMicroelectronics Imaging Division, 33 Pinkhill, Edinburgh, UK, EH12 7BF; <sup>[5]</sup>Dialog Semiconductor (UK) Ltd.,

<sup>[6]</sup>Institute of Microstructure Technology (IMT), Karlsruhe Institute of Technology (KIT), 76131 Karlsruhe, Germany  
[andreas.eisele@de.bosch.com](mailto:andreas.eisele@de.bosch.com) Tel: +49 711 758-3364 Fax: +49 711 811-5184731

**Abstract** – Single-photon avalanche diodes with active and passive quenching circuits are fabricated on a 130 nm CMOS platform and analyzed with respect to saturation behavior at high photon rates.

## I. INTRODUCTION

Single-photon avalanche diodes (SPAD) are successfully employed for low-light level, time-correlating applications such as fluorescence lifetime imaging (FLIM) [1], fluorescence correlation spectroscopy (FCS), and positron emission tomography (PET). However, the saturation of these detectors at high firing frequency (count rate) constitutes the upper limit for the detector dynamic range and remains a problem for measurements in bright sunlight.

In this paper, we discuss a special form of saturation, namely the “paralysis” of a SPAD, and we provide a solution to the problem. The count rate of a paralyzed detector decreases nonlinearly with increasing incident illumination [2].

This effect has serious implications for applications such as 3D range imagers [3], which demand high dynamic range and *monotonously* increasing count rate. Furthermore we demonstrate that by employing a compact active quenching circuit [4], co-integrated with a SPAD in 130 nm CMOS technology [5], we achieve a *non-paralyzable* maximum count rate of 185 MHz, and a dynamic range of 139 dB at a low afterpulsing probability of 1.28 %. Comparing to state-of-the-art results [6], the dynamic range is improved by 6 dB, and the count rate is increased by a factor of 3.

## II. CIRCUIT OPERATION

In a passively quenching configuration (Fig. 1a), the SPAD is biased with an excess bias voltage above the breakdown voltage,  $V_{eb} > V_{br}$ . An incident photon triggers an avalanche. The avalanche current reduces the SPAD voltage  $V_S$  below breakdown, Fig. 2a. The resistor  $R$  recharges the junction

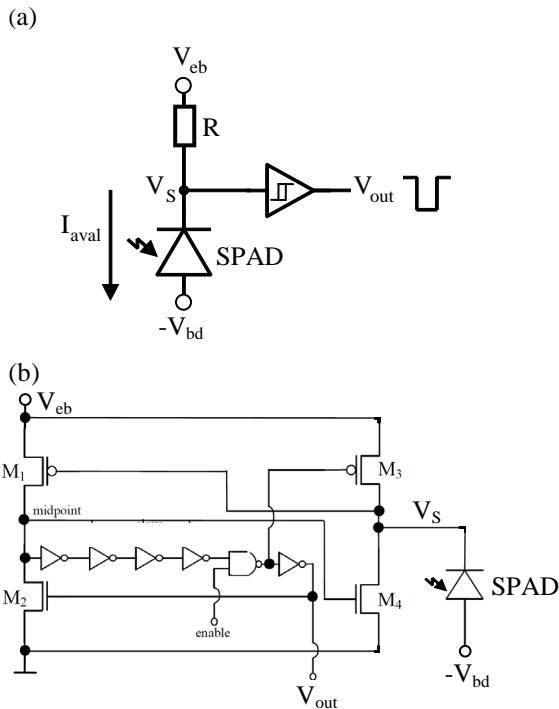


Fig. 1: Quenching circuits. (a) Passive circuit; signal detector with threshold  $V_{th}$ , (b) active monostable circuit; threshold fixed by gate voltage for switching transistor  $M_1$  to on-state

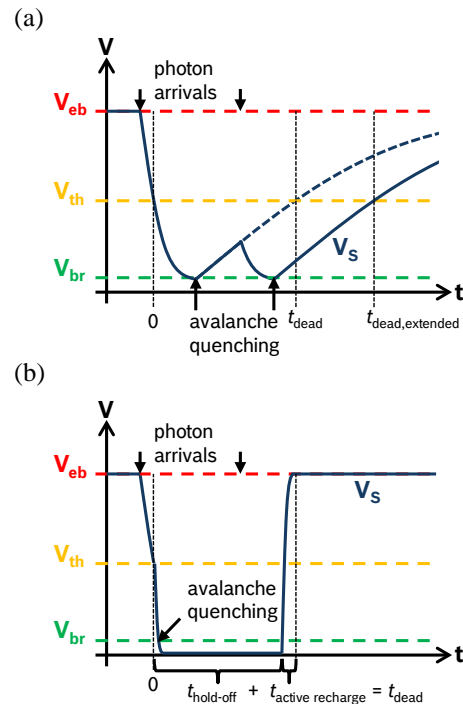


Fig. 2: SPAD voltage  $V_S$  and dead time  $t_{dead}$  (a) Another photon incident during dead time can extend the dead time of the passive quenching circuit to  $t_{dead,extended}$ . (b) The active quenching circuit does not suffer from dead time extensions.

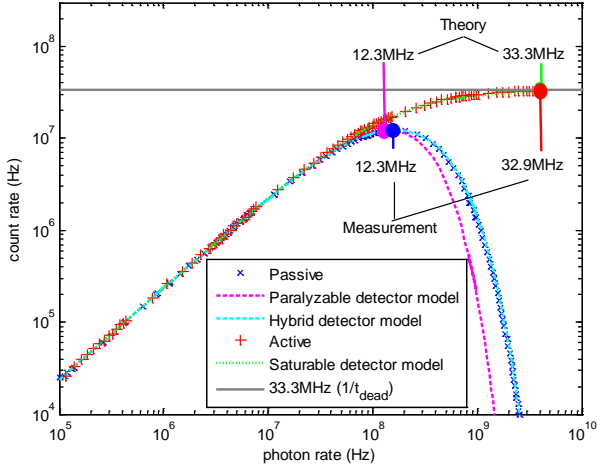


Fig. 3: Sensitivity measurements for fabricated passive and active quenching circuits in comparison with a paralyzable, hybrid and saturable detector model [8]. Dead time 30 ns, excess bias 1.80 V. Hybrid model fit to measurement data with 21 ns non-paralyzable and 14 ns paralyzable dead time.

capacitance and other parasitic capacitances. As soon as  $V_{br}$  is exceeded, the SPAD can be triggered by another photon. As a consequence,  $V_S$  can remain below the threshold voltage of the trigger circuit  $V_{th}$ , such extending the dead time and “paralyzing” the photon detection.

The relation between measured count rate  $m$  and the true count rate  $n$  for a dead time  $t_{dead}$  can be predicted by a paralyzable-detector model adopted from nuclear particle physics instruments [2],

$$m = n \cdot e^{-n \cdot t_{dead}}. \quad (1)$$

A photon incident during avalanche discharge does not paralyze the device, because a photo-generated electron-hole pair only adds to an already existing avalanche. This is taken into account by the hybrid deadtime model [8,9]

$$m = \frac{n \cdot e^{-n \cdot t_{dead, paralyzable}}}{1 + n \cdot t_{dead, saturable}}. \quad (2)$$

In an actively quenching configuration (Fig. 1b), the SPAD voltage  $V_S$  is reduced below  $V_{br}$  by a monostable positive-feedback circuit, the time constant of which (hold-off time in Fig. 2b) is adjusted by the rise times of the inverters connected to transistor  $M_2$  [4], so preventing premature SPAD breakdown. When the quenching circuit switches back to its stable state,  $M_3$  represents a low resistance and rapidly recharges the SPAD, even when the SPAD fires during the recharging process. The count rate can be predicted by the relation

$$m = \frac{n}{1 + n \cdot t_{dead}}. \quad (3)$$

The count rate eventually saturates at  $1/t_{dead}$  for high photon rates.

So-called afterpulses [7] are caused by internally discharging the SPAD, but occur with reduced probability because of the rapid discharge circuit external to the SPAD. This is expected to reduce afterpulsing especially for larger active area SPADs (Fig. 5a) with larger capacitance and

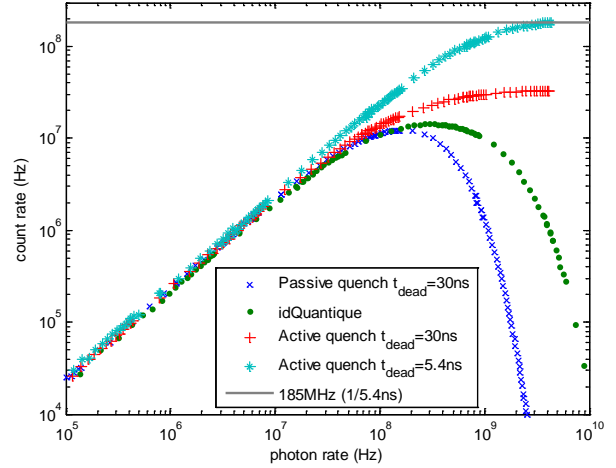


Fig. 4: Sensitivity measurements for a fabricated passive quenching circuit, a commercially available active quenching SPAD (idQuantique id101-20), and a fabricated active quenching circuit. At 5.4 ns dead time, the active quench SPAD is operated at 2.6V excess bias.

defect probability because the bypass through  $M_4$  reduces the charge flow through the SPAD pn-junction.

### III. EXPERIMENTAL RESULTS

We investigate two SPAD configurations with 8  $\mu\text{m}$  diameter circular active area, Fig. 5. Both are illuminated with the well-defined irradiance of a red LED having a center wavelength of 638 nm, Fig. 3.

The active quenching circuit actually reaches the theoretical saturation count rate of  $1/t_{dead}$ . The peak count rate of the passive quenching is accurately predicted via the paralyzable-detector model by  $1/(\exp(1) \cdot t_{dead})$ , however the measured count rate deviates from the idealized model at high photon rates. The hybrid detector model fits the measured passive quenching count rates. However, the sum of paralyzable and saturable fitted dead times exceeds the measured 30 ns dead time by 5 ns. This deviation cannot be explained by either detector model because SPAD recharge effects are not taken into account. As the photon detection efficiency (PDE) recovers with increasing  $V_{eb}$ , the probability of triggering another avalanche shortly after avalanche quenching is reduced. This results in a lower effective photon rate seen by the detector, and it translates to an under-estimated count rate at high photon rates in the paralyzable detector model, or to an inaccurate dead time in the hybrid detector model. For accurate predictions, SPAD pulse voltage curves and PDE dependence on  $V_{eb}$  must be taken into account.

For a dead time of 5.4 ns and an excess bias of 2.6 V, the actively quenched SPAD reaches a maximum count rate of 185 MHz, Fig. 4. The dynamic range is  $20 \log_{10}[(\text{maximum count rate}) / (\text{RMS dark count rate})] = 139 \text{ dB}$ . A commercially available SPAD (idQuantique id101-20) is measured as a reference. Note that this device shows paralyzable behavior despite its active quenching circuit. In this work a powerful recharge transistor  $M_3$  (Fig. 1b) prevents paralysis during recharge.

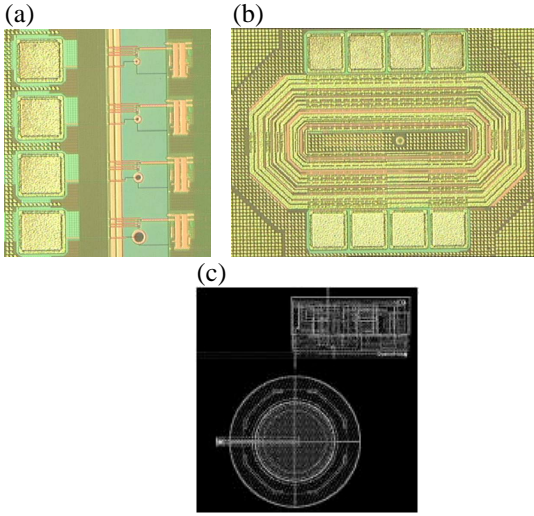


Fig. 5: Photomicrographs of (a) passive quenching cells with different SPAD active areas, (b) active quenching cell for the -SPAD of Fig. 5c, (c) actively quenched disk-shaped SPAD with 8  $\mu\text{m}$  diameter and associated 8  $\mu\text{m}$   $\times$  17  $\mu\text{m}$  active quenching circuit

Afterpulsing is analyzed in darkness to resolve even faint afterpulses exceeding the rare random dark counts at low noise. A LeCroy 20 GSa/s oscilloscope running a custom-made signal processing function overcomes trace length limitations of the instrument’s inbuilt autocorrelation analysis. SPAD pulse arrival times are evaluated and displayed in form of a histogram under the assumption that an event has actually occurred at time zero. The analysis is equivalent to an autocorrelation [10].

The result is displayed as a conditional probability density function (Fig. 6). Table 1 provides a performance summary.

#### IV. CONCLUSION

We presented single-photon avalanche diodes with both active and passive quenching circuits. While identical count rates are measured at low light levels, the actively quenched SPAD shows superior performance at high incident illumination exhibiting a monotonously increasing count rate.

A count rate of 185 MHz and a dynamic range of 139 dB, represent, to the best of our knowledge, the highest count rate and dynamic range for single-photon avalanche diodes reported so far.

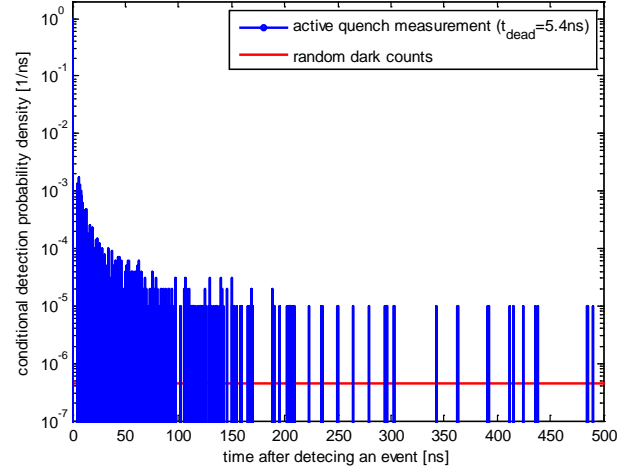


Fig. 6: Conditional detection probability density function (PDF) of a detection event, provided a photon has been detected at time 0. Integration over the PDF from 5 ns to 275 ns gives 1.28 % afterpulse probability in addition to the dark count probability.

#### REFERENCES

- [1] D. U. Li, J. Arlt, J. Richardson, R. Walker, A. Buts, D. Stoppa, E. Charbon, R. K. Henderson, “Real-time fluorescence lifetime imaging system with a  $32 \times 32$  0.13 $\mu\text{m}$  CMOS low dark-count single-photon avalanche diode array”, *Optics Expr.*, Vol. 18, Issue 10, pp.10257-10269, 2010.
- [2] W. R. Leo, “Techniques for nuclear and particle physics experiments”, Springer, pp.122-124, 1994
- [3] C. Niclass, E. Charbon, “A single photon detector array with  $64 \times 64$  resolution and millimetric depth accuracy for 3D imaging”, *ISSCC*, pp. 364-365, 2005
- [4] J. Richardson, R. K. Henderson, D. Renshaw, “Dynamic quenching for single photon avalanche diode arrays”, *IISW*, 2007
- [5] J. Richardson, L. A. Grant, R.K. Henderson, “A low dark count single photon avalanche diode structure compatible with standard nanometer scale CMOS technology”, *IISW*, 2009
- [6] C. Niclass, M. Soga, “A miniature actively recharged single-photon detector free of afterpulsing effects with 6ns dead time in a 0.18 $\mu\text{m}$  CMOS technology”, *IEDM*, 2010
- [7] S. Cova, M. Ghioni, A. Lacaita, C. Samori, F. Zappa, “Avalanche photodiodes and quenching circuits for single-photon detection”, *Applied Optics*, Vol. 35, Issue 12, pp. 1956-1976, 1996
- [8] S. Lee, R. Gardner, “A new G-M counter dead time model”, *Applied Radiation and Isotopes*, 53, 731-737, 2000
- [9] L. Neri, F. Musumeci, A. Scordino, G. Fallica, M. Mazzillo, M. Zimbone “Dead time causes and correction method for single photon avalanche diode devices”, *Review of Scientific Instrumentation*, 81, 086102, 2010
- [10] W.J. Kindt, “Geiger mode avalanche photodiode arrays”, PhD-Thesis, TU Delft, 1999

TABLE I: PERFORMANCE SUMMARY

Device	Excess bias $V_{\text{eb}}$	Dead Time $t_{\text{dead}}$	Dark Count Rate* (DCR)	Poisson RMS DCR* ( $\sqrt{\text{DCR}}$ )	Maximum Count Rate $C_{\text{max}}$	Dynamic Range** $\frac{C_{\text{max}}}{\sqrt{\text{DCR}}}$	Afterpulse Probability ( $\pm 1 \sigma$ )
	[V]	[ns]	[Hz]	[(Hz) <sup>1/2</sup> ]	[MHz]	[dB]	[%]
idQuantique	-	39	374.0	19.3	14.4	117.4	0.523 ( $\pm 0.135$ )
Passive	1.8	30	153.0	12.4	12.3	119.9	0.567 ( $\pm 0.076$ )
Active	1.8	30	110.0	10.5	32.9	129.9	0.428 ( $\pm 0.064$ )
Active	2.6	5.4	410.8	20.3	185.0	139.2	1.28 ( $\pm 0.036$ )

\* at room temperature

\*\* Dynamic range =  $20 \log_{10} \left( \frac{C_{\text{max}}}{\sqrt{\text{DCR}}} \right)$ . Acquisition time is 1 s